Supplemental information for

IFITM proteins promote SARS-CoV-2 infection and are targets for virus inhibition

Caterina Prelli Bozzo[1#], Rayhane Nchioua[1#], Meta Volcic[1], Jana Krüger[2], Sandra Heller[2], Christina M. Stürzel[1], Dorota Kmiec[1,3], Carina Conzelmann[1], Janis Müller[1], Fabian Zech[1], Desiree Schütz[1], Lennart Koepke[1], Elisabeth Braun[1], Rüdiger Groß[1], Lukas Wettstein[1], Tatjana Weil[1], Johanna Weiß[1], Daniel Sauter[1,4], Jan Münch[1], Federica Diofano[5], Christine Goffinet[6], Alberto Catanese[7], Michael Schön[7], Tobias Böckers[7], Steffen Stenger[8], Kei Sato[9], Steffen Just[5], Alexander Kleger[2], Konstantin M.J. Sparrer[1*] and Frank Kirchhoff[1*]

[1]Institute of Molecular Virology, Ulm University Medical Centre, 89081 Ulm, Germany. [2]Department of Internal Medicine I, Ulm University Medical Centre, 89081 Ulm, Germany. [3]Department of Infectious Diseases, King's College London, WC2R 2LS London, United Kingdom. [4]Institute of Medical Virology and Epidemiology of Viral Diseases, University Hospital Tübingen, 72076 Tübingen, Germany. [5]Department of Internal Medicine II (Cardiology), Ulm University, 89081 Ulm, Germany. [6]Institute of Virology, Charité - Universitätsmedizin Berlin, 10117 Berlin, Germany. [7]Institute for Anatomy and Cell Biology, Ulm University, 89081 Ulm Germany. [8]Institute of Medical Microbiology and Hygiene, Ulm University Medical Centre, 89081 Ulm, Germany. [9]Institute of Medical Science, The University of Tokyo, 1088639 Tokyo, Japan.

* Correspondence: konstantin.sparrer@uni-ulm.de or Frank.Kirchhoff@uni-ulm.de
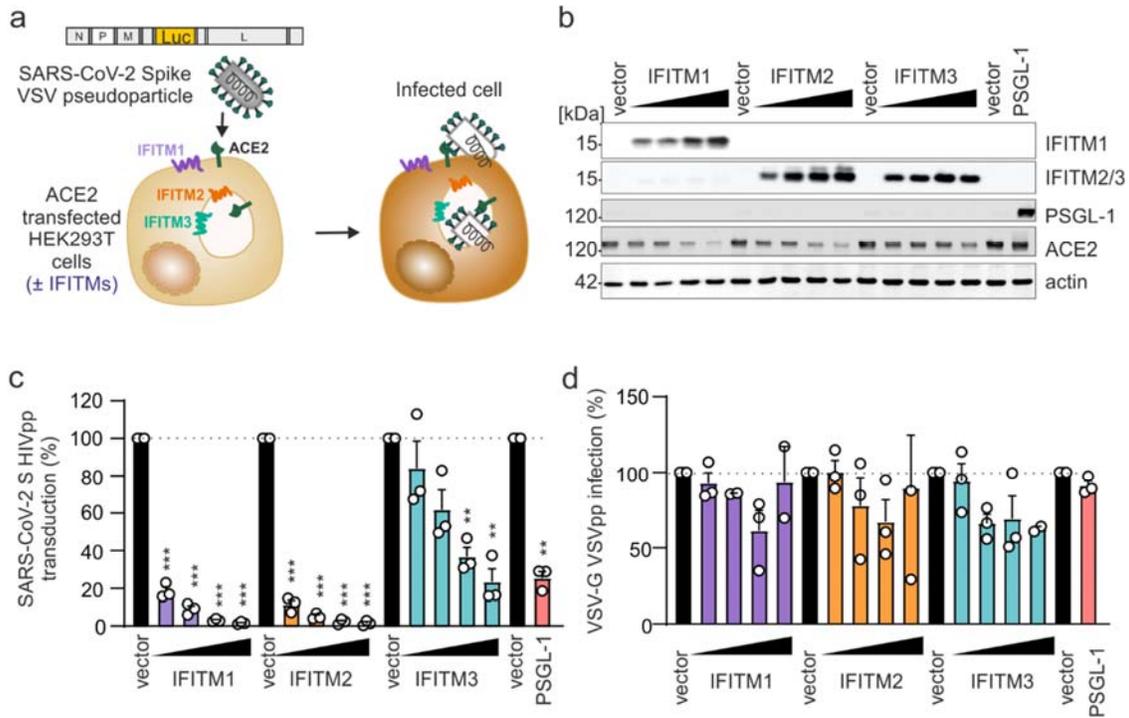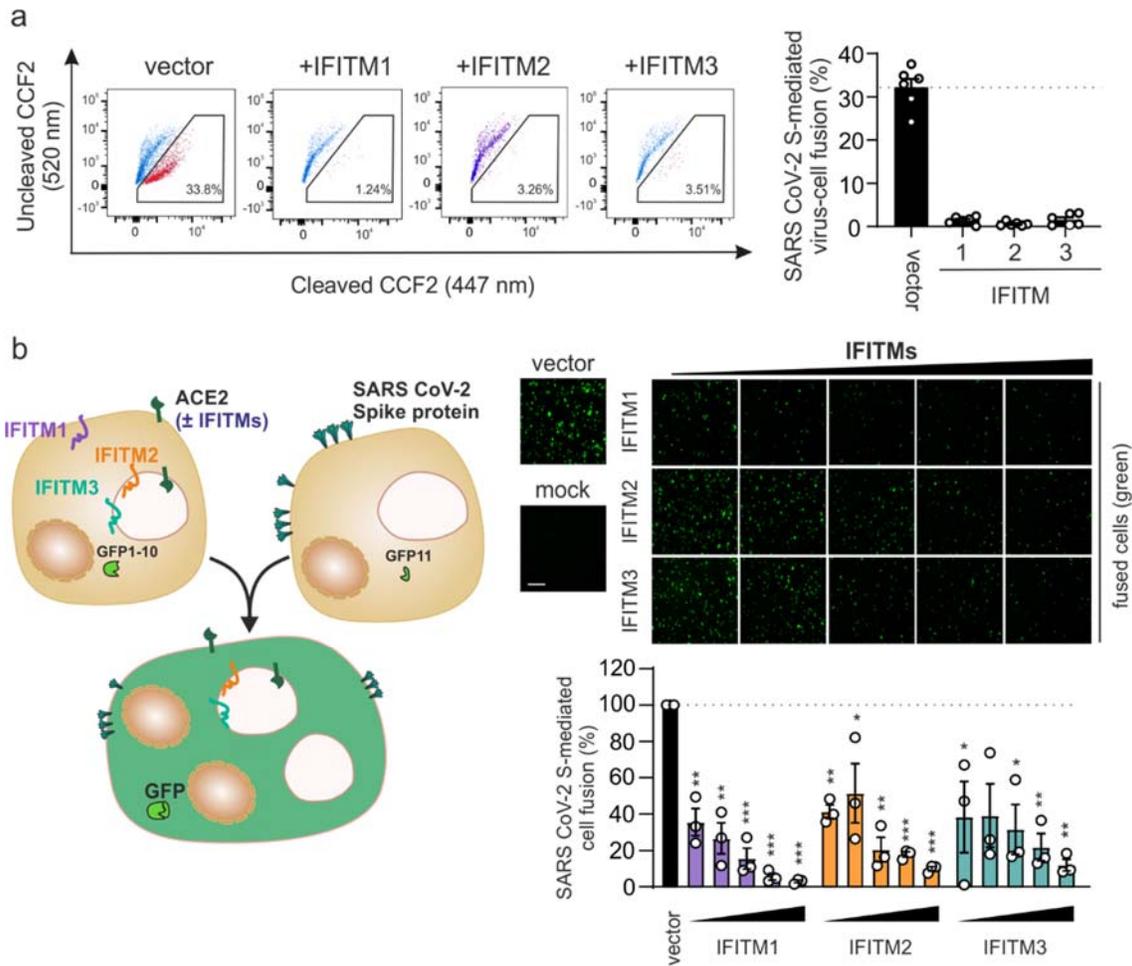
Extended data Figure 1. Effect of IFITM overexpression on Spike- or VSV-G-mediated pseudoparticle infection. a, Schematic depiction of the assay to assess VSVpp entry. **b**, Immunoblot of whole cell lysates (WCLs) of HEK293T cells co-transfected with expression plasmids for ACE2, empty or PSGL-1 expressing control vectors, or different doses of IFITM expression constructs. Immunoblots of whole cell lysates were stained with anti-IFITM1, anti-IFITM2, anti-IFITM3 and anti-actin. **c,** Quantification of SARS-CoV-2-S-mediated entry by measuring luciferase activity in HEK293T cells transiently transfected with the indicated expression vectors and transduced 24 h post-transfection with HIV(luc)Δ*env**-SARS-CoV-2 S for 48 h. All bar diagrams in this figure represent means of n=3 (±SEM). PSGL-1 was recently shown to block SARS-CoV-2 attachment[45] and was used as positive control for inhibition. **d**, VSV(luc)ΔG*VSV-G entry in HEK293T cells transiently expressing indicated proteins and infected 24 h post transfection with VSV(luc) ΔG*VSV-G (MOI 0.025) for 16 h. Lower panel: Immunoblot of the corresponding whole cell lysates (WCLs) stained with anti-IFITM1, anti-IFITM2, anti-IFITM3, anti-PSGL-1, anti-ACE2 and anti-actin.
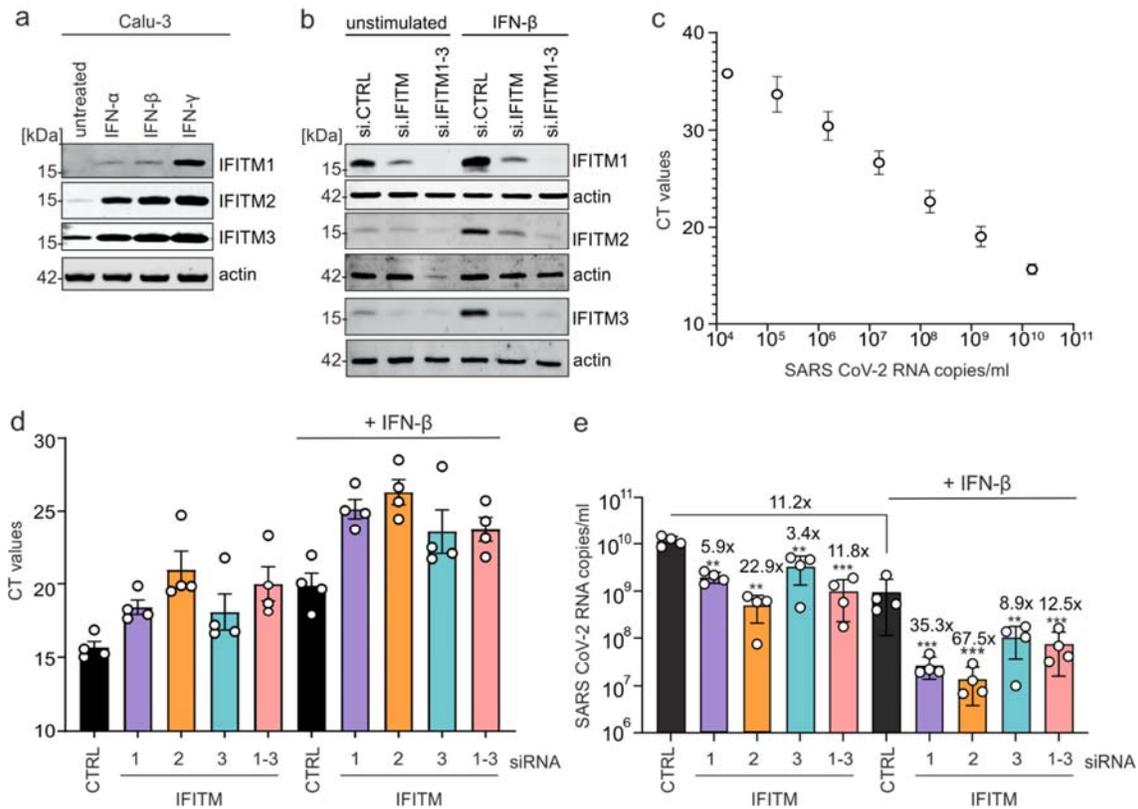
Extended data Figure 2. Impact of IFITM siRNA knock-down on SARS-CoV-2 replication in Calu-3 cells. **a**, Expression of IFITM1, IFITM2 and IFITM3 in Calu-3 cells after stimulation with IFN-α2 (500 U/ml, 72 h), IFN-β (500 U/ml, 72 h) or IFN-γ (200 U/ml, 72 h). Immunoblots of whole cell lysates were incubated with anti-IFITM1, anti-IFITM2, anti-IFITM3 and anti-actin. **b**, Expression of IFITM proteins in Calu-3 cells transfected with non-targeting or IFITM-specific siRNAs. Cells were either stimulated with IFN-β (500 U/ml, 72 h) or left untreated. Immunoblots of whole cell lysates were stained with anti-IFITM1, anti-IFITM2, anti-IFITM3 and anti-actin. **c**, Standard curve, **d**, raw qRT-PCR CT values and **e**, SARS-CoV-2 RNA copy numbers in the supernatant of Calu-3 cells collected 2 days post-infection with SARS-CoV-2 (MOI 0.05). Relative levels of viral RNA production and shown in Figure 1d. Number above the bars indicate n-fold reduction of viral RNA levels upon knockdown of the respective IFITM proteins compared to cells treated with control siRNA or fold inhibit by IFN-β treatment, respectively. The bar diagram shows mean values (+/SD) from four independent experiments each measured in technical duplicates.
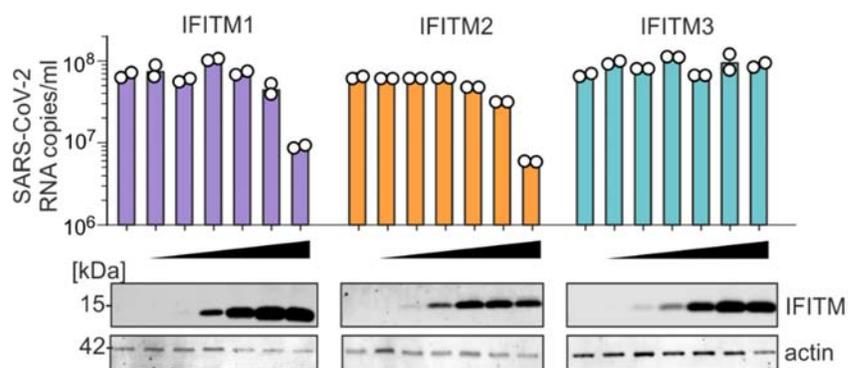
Extended data Figure 3. Effect of different levels of transient IFITM expression on SARS-CoV-2 infection. SARS-CoV-2 RNA production from HEK239T cells transiently expressing ACE2 and increasing levels of the indicated IFITM proteins. Quantification of viral N gene RNA by qRT-PCR in the supernatant of HEK293T was performed 48 h post-infection with SARS-CoV-2 (MOI 0.05). Bars represent means of n=2±SEM.
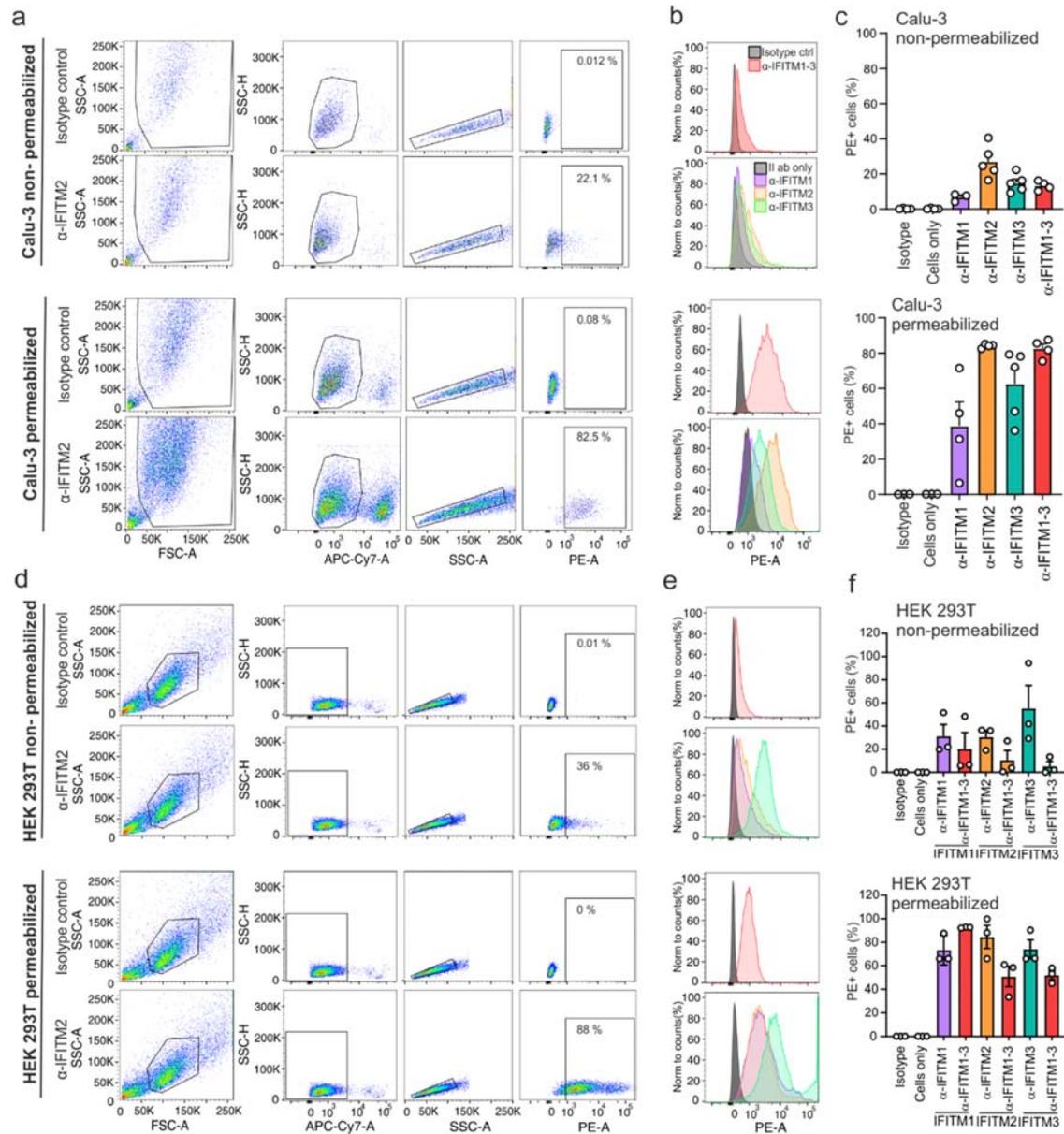
Extended data Figure 4. Overexpression of IFITMs prevents S-mediated virion and cell-to-cell fusion. a, Fusion of HIV(Vpr-Blam)Δ*env**-SARS-CoV-2-S with HEK293T cells transiently expressing ACE2 and IFITMs. Quantification of the fusion efficiency by flow cytometry as percentage of (cleaved CCF2) positive cells. Bars represent means (±SEM) of three experiments each done in triplicate. Right panel: Exemplary gating of the raw data. **b**, Schematic outline of the split-GFP assay measuring cell-cell fusion (left). GFP1-11 and SARS-CoV-2 Spike expressing HEK293T were co-cultured with GFP10, ACE2 and IFITM expressing HEK293T. Exemplary fluorescence images (upper). Quantification of successful fusion by GFP positive cells (green) normalized to nuclei (lower right). Bars represent means of n=3, ±SEM.
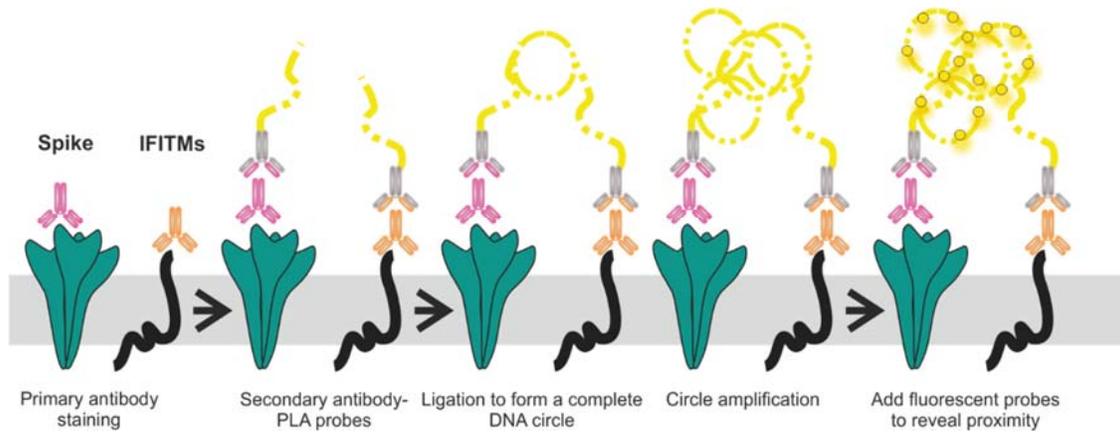
Extended data Figure 5. Schematic outline of the Proximity ligation assay (PLA). This assay measures the proximity between SARS-CoV-2 Spike protein and the IFITMs proteins.
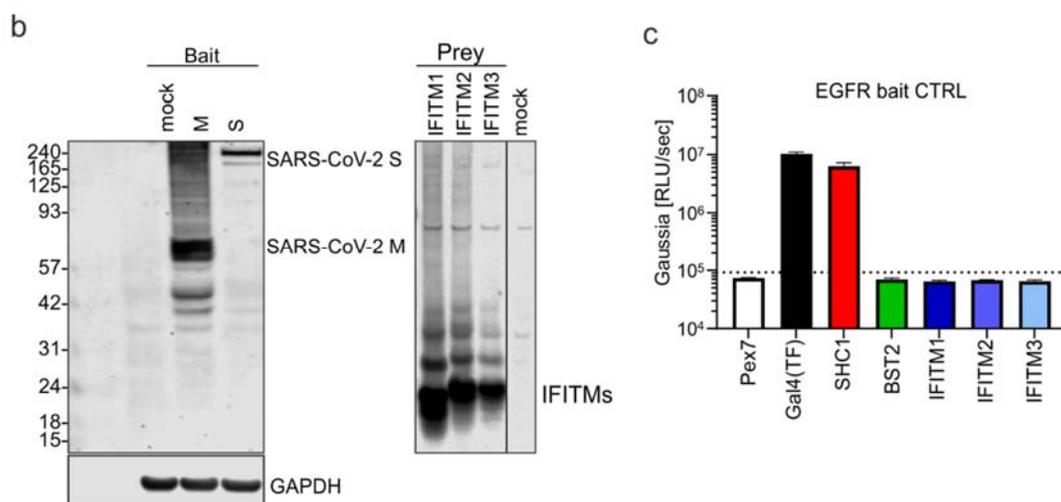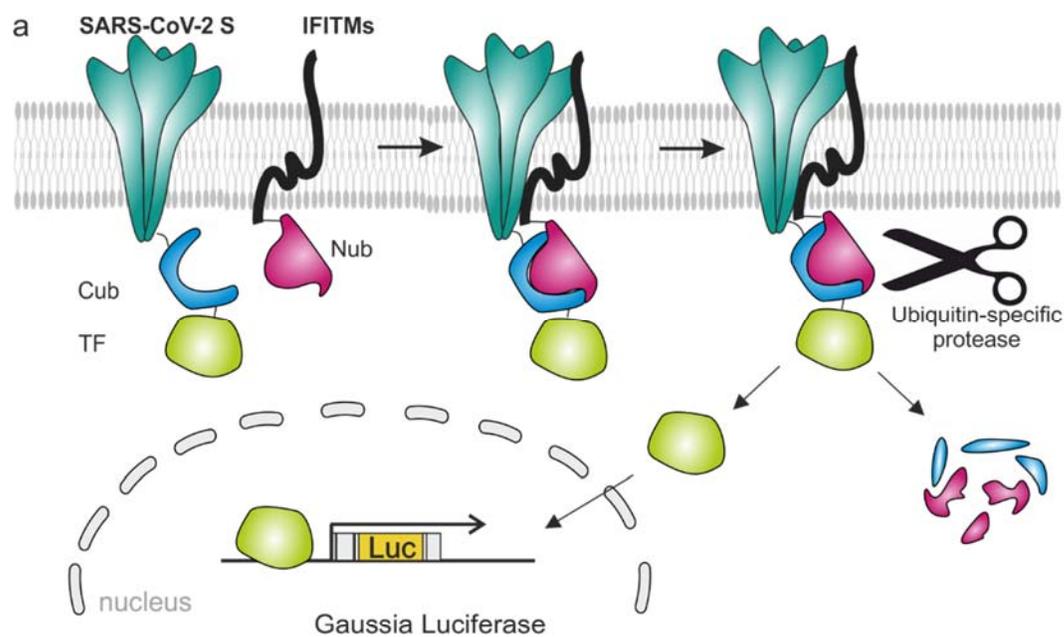
Extended data Figure 6. Analysis of protein-protein interactions by MaMTH assay. a, Schematic representation of the MaMTH assay measuring interaction between SARS-CoV-2 Spike and IFITM1, 2 or 3. **b,** Western blot showing the expression of MaMTH V5-tagged SARS-CoV-2 protein Baits and FLAG-tagged IFITM Preys in transfected HEK293T B0166 cells. GAPDH shown as loading control. **c,** Raw values of negative (Baits only or Preys with EGFR Bait) and positive controls (transcription factor Gal4 or EGFR with SHC1) used in MaMTH protein-protein interaction assay. Dotted line indicates untransfected sample value (mock). Mean of triplicate transfection + SD.

Extended data Figure 7. Flow cytometric analysis of IFITM expression. a, Gating strategy and flow cytometric detection of endogenous IFITMs in non-permeabilized (upper) or permeabilized (lower) Calu-3 cells using α-IFITM1, α-IFITM2, α-IFITM3 and α-IFITM1-3 antibodies. The left part shows examples for primary data and the bar diagrams quantitative results from the FACS analyses. **b and e,** Histograms represent the percentage of positive cells normalized for alive/single cells. **c,** Bars represent four independent experiments (±SEM) **d,** flow cytometric analyses of non-permeabilized (upper) or permeabilized (lower) HEK293T cells transiently transfected with constructs expressing the indicated IFITM proteins and analyzed using the corresponding α-IFITM1, α-IFITM2, α-IFITM3 or α-IFITM1-3, respectively. **f,** Bars represent three independent experiments (±SEM)

8
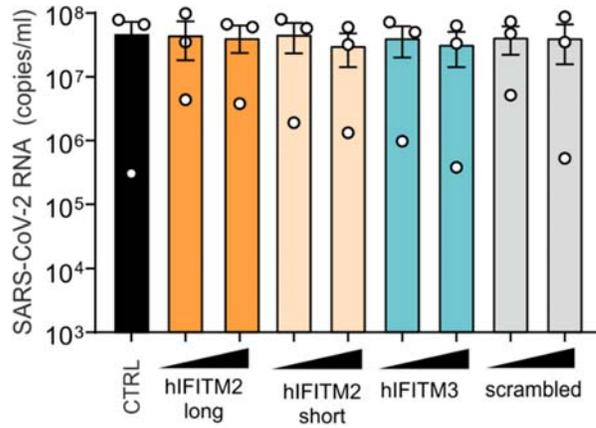
Extended data Figure 8. Effect of IFITM-derived peptides on SARS-CoV-2 infectivity.
Viral N gene RNA levels in the supernatant of Calu-3 cells infected with SARS-CoV-2 pre-treated with two concentrations of IFITM-derived peptides. Bars represent two independent experiments measured in technical duplicates (mean, ±SEM).
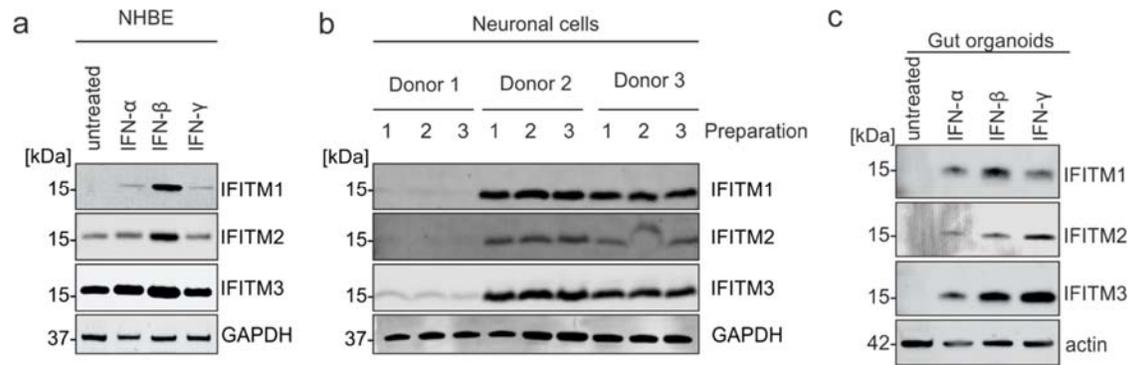
Extended data Figure 9. Expression of IFITMs in primary lung cells, neuronal cells and gut organoids. a, Expression of IFITM1, IFITM2 and IFITM3 in primary bronchial epithelial cells (NHBE) after stimulation with IFN-α2 (500 U/ml, 72 h), IFN-β (500 U/ml, 72 h) or IFN-γ (200 U/ml, 72 h). Immunoblot of whole cell lysates stained with anti-IFITM1, anti-IFITM2, anti-IFITM3 and anti-GAPDH. **b,** Expression of IFITM1, IFITM2 and IFITM3 in neuronal cells. Cell lysates have been prepared from three independent differentiations of induced pluripotent stem cells of three different donors. **c**, Expression of IFITM1, IFITM2 and IFITM3 after stimulation with IFN-α2 (500 U/ml, 72 h), IFN-β (500 U/ml, 72 h) or IFN-γ (200 U/ml, 72 h) in stem cell derived gut organoids.
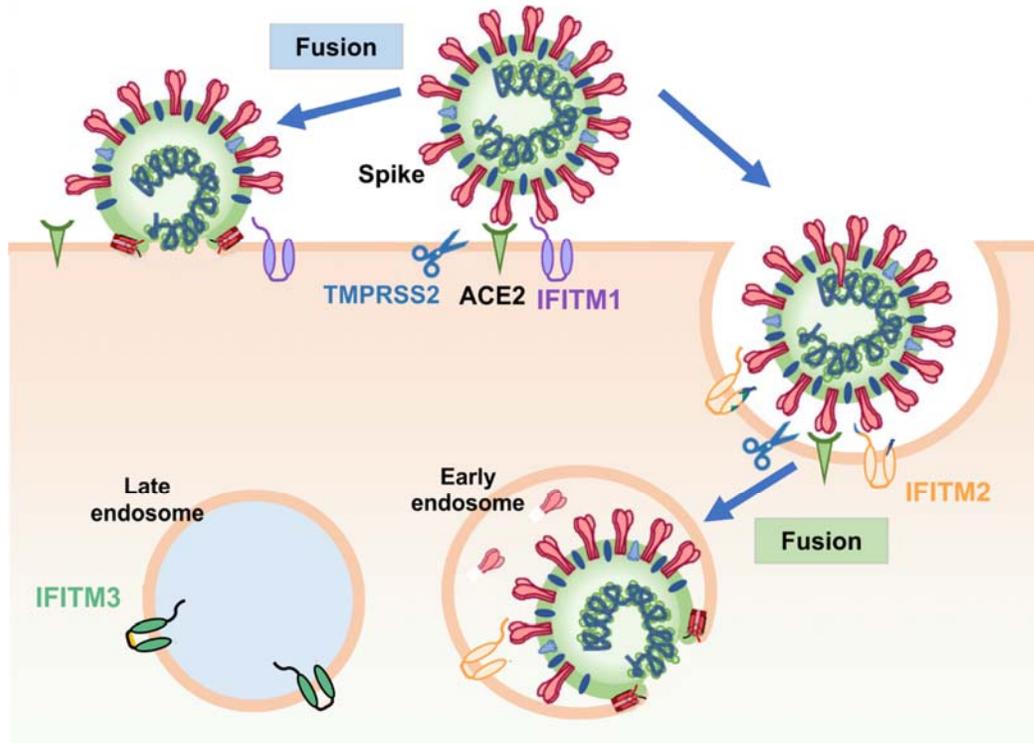
Extended data Figure 10. Schematic presentation of the potential role of IFITM protein in SARS CoV-2 infection. Modified from Ref. 24.